

Disassembling the Dataset: A Camera Alignment Mechanism for Multiple Tasks in Person Re-identification

Zijie Zhuang¹ Longhui Wei² Lingxi Xie² Hengheng Zhang³
 Tianyu Zhang² Haozhe Wu¹ Haizhou Ai¹ Qi Tian²
¹Tsinghua University ²Huawei Noah's Ark Lab ³Hefei University of Technology

jayzhuang42@gmail.com weilh2568@gmail.com 198808xc@gmail.com imhnmh@gmail.com
 tianyu1949@gmail.com wuhz1997@163.com ahz@tsinghua.edu.cn tian.qil@huawei.com

Abstract

In person re-identification (ReID), one of the main challenges is the distribution inconsistency among different datasets. Previous researchers have defined several seemingly individual topics, such as fully supervised learning, direct transfer, domain adaptation, and incremental learning, each with different settings of training and testing scenarios. These topics are designed in a dataset-wise manner, i.e., images from the same dataset, even from disjoint cameras, are presumed to follow the same distribution. However, such distribution is coarse and training-set-specific, and the ReID knowledge learned in such manner works well only on the corresponding scenarios. To address this issue, we propose a fine-grained distribution alignment formulation, which disassembles the dataset and aligns all training and testing cameras. It connects all topics above and guarantees that ReID knowledge is always learned, accumulated, and verified in the aligned distributions. In practice, we devise the Camera-based Batch Normalization, which is easy for integration and nearly cost-free for existing ReID methods. Extensive experiments on the above four ReID tasks demonstrate the superiority of our approach. The code will be publicly available.

1. Introduction

Person re-identification (ReID) aims at matching identities across disjoint cameras. Generally, due to the huge appearance variations caused by illumination conditions, camera views, etc., images from different datasets are subject to distinct distributions, as shown in Fig. 1(a).

To handle the potential distribution shift among datasets, researchers have defined several seemingly individual topics, each with different regularization of training and testing scenarios: (1) the fully supervised learning [1, 44, 34, 46, 47, 51] handles the scenario in which the train-

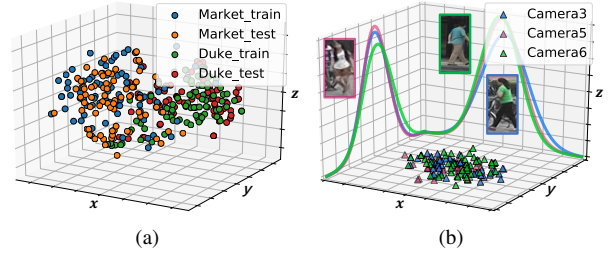


Figure 1. (a) Barnes-Hut t-SNE [37] visualizations of the distribution inconsistency among datasets. (b) We visualize the distributions of several cameras in Market-1501. The curve corresponds to the approximated marginal density function. Curves of different cameras demonstrate noticeable differences. Best viewed in color.

ing data and testing data are sampled from the same distribution; (2) the direct transfer [21, 8] tries to learn the generalized knowledge from the training distribution and apply it to any other distributions; (3) the domain adaptation [39, 3, 50, 4, 31, 45] learns the knowledge from one labeled source distribution and leverages it to guide the learning process on another unlabeled target distribution; (4) finally, in incremental learning [27, 16, 12], researchers sequentially fine-tune the model on multiple training datasets, trying to preserve the knowledge learned from all distributions simultaneously. Apparently, all these topics are organized in a dataset-wise manner, and we denote such manner as the conventional dataset-based formulation. With such formulation, all topics above need to estimate the dataset-wise distribution, which is not only coarse but also imposes a hurdle for transferring the knowledge across datasets. As a consequence, the knowledge learned for different dataset combinations is isolated, resulting in the difficulty of connecting all these ReID topics.

In this paper, we connect these isolated topics with a more generic formulation. Specifically, we propose to explicitly align the distributions of training and testing datasets in a fine-grained manner, so that the ReID knowl-

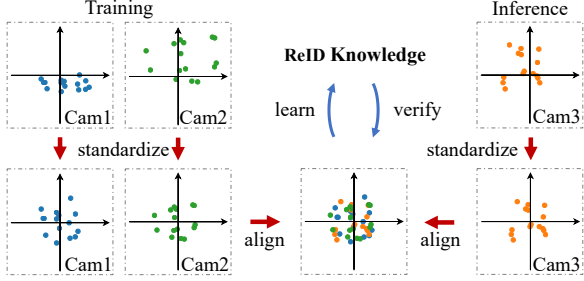


Figure 2. Demonstrations of the proposed camera-based formulation. It explicitly aligns the distribution of each training and testing camera. This approach ensures that ReID knowledge is always learned, accumulated, and verified in the aligned distributions.

edge can always be learned, accumulated, and verified in similar distributions. As indicated by some previous works [39, 3, 50], the image style in different cameras varies even in the same dataset. The variations among cameras further lead to the distribution inconsistency inside the dataset, as demonstrated in Fig. 1(b). Therefore, we propose a novel camera-based formulation that learns ReID knowledge in a camera-wise manner. As shown in Fig. 2, aligning the distributions of all cameras enables us to always learn and verify the ReID knowledge in similar distributions, which is beneficial to transfer the knowledge across all datasets.

To implement this formulation, we need a straightforward mechanism for explicitly aligning the distribution of each camera. For deep neural networks, an off-the-shelf solution without preconceiving the distribution of deep features is Z-score standardization, which has already been integrated into numerous deep neural networks via Batch Normalization (BN) [9]. We take advantage of this fact and adjust the standardization process inside BN layers for aligning the distributions of all training and testing cameras. We name this modified version of BN as Camera-based Batch Normalization (CBN) and utilize it for improving all aforementioned ReID tasks. During training, CBN layers record the statistics of their input and standardize them per camera. In the inference stage, CBN layers approximate the camera-related statistics with a few unlabeled images from each testing camera, then use these statistics to align the distributions of testing cameras and generate the final features. With this simple modification, the learned knowledge is well generalized across all aligned datasets. Extensive experiments indicate that our method improves the performance of multiple ReID tasks simultaneously, such as 0.9%, 5.7%, and 14.2% averaged rank-1 accuracy improvements on fully supervised learning, domain adaptation, and direct transfer, respectively, and 9.7% less forgetting on rank-1 accuracy for incremental learning. Meanwhile, the proposed CBN layer is easy to implement and nearly cost-free. To conclude, our contribution is three-fold:

- This paper reveals the inherent cause that isolates ReID

topics and emphasizes that explicitly aligning the distribution of all cameras is a generic solution to connect and improve all ReID topics mentioned above.

- We propose a camera-based formulation and implement it through Camera-based Batch Normalization. Without bells and whistles, our method boosts the performance on multiple ReID tasks simultaneously.
- Our formulation provides a new perspective for designing and deploying ReID algorithms. It paves a new way for future researches in ReID.

2. Related Work

Our formulation works by aligning the distribution per camera. It handles an arbitrary number of training cameras and testing cameras. Besides, it is not sensitive to whether the testing cameras exist in training datasets. Therefore, our formulation covers the common scenarios for many ReID tasks, *e.g.*, fully supervised learning, direct transfer, domain adaptation, and incremental learning. In this section, we briefly summarize previous works on these tasks.

Fully Supervised Learning is the task in which all training images have human annotations, and testing images are sampled from the same scene as training images. Lots of methods [1, 44, 34, 46, 47, 51, 11, 40] were proposed to generate discriminative features. Many of them designed spatial alignment [42, 35, 32], visual attention [13, 19], semantic segmentation [11, 36, 29] for extracting accurate and fine-grained features. Meanwhile, some works [20, 10, 22] utilized GAN-based methods for data augmentation, which hugely improve the ReID performance.

Direct Transfer. Although the works above achieve excellent performance on fully supervised learning, they usually perform poorly in unseen scenes [30, 39, 3]. This phenomenon is referred to as domain gap and attracts the attention of ReID community. To evaluate the robustness of ReID algorithms, researchers proposed the direct transfer task, in which the testing images are sampled from the previously unseen cameras. To improve the generalization ability, various strategies are adopted as additional constraints to avoid over-fitting, such as label smoothing [21] and sophisticated part alignment approaches [8].

Domain Adaptation is the task of transferring knowledge from labeled source domains to target domains, where target domains lack human annotations. One solution is to generate fake training images for target domains, *e.g.*, PT-GAN [39], SPGAN [3], and CamStyle [50] utilized CycleGAN [52] to transfer image styles from source to target. Meanwhile, other methods try to utilize the semantic knowledge encoded in the learned models [6, 38, 4, 17]. Song *et al.* [31] utilized the pre-trained ReID model to generate pseudo labels. ECN [49] analyzed the intra-domain variations and proposed an exemplar memory for the target data.

Incremental Learning is a popular topic in machine learning [27, 16, 12] but rarely discussed in the ReID community. The goal of incremental learning is to preserve previous knowledge while learning the new one. This task is vital for ReID, especially when only part of the training set is available at a time. A recent ReID work that relates to incremental learning is MASDF [41], which distilled and incorporated the knowledge from multiple datasets.

3. Methodology

3.1. Overview

Basic Formulation. Given an image $\mathbf{I}_i^{\mathcal{D}_j}$ from any training set \mathcal{D}_j , the training goal of the conventional dataset-based formulation is:

$$\arg \min \mathbb{E} \left[\mathbf{y}_i^{\mathcal{D}_j} - \mathbf{g}^{\mathcal{D}_j} \left(\mathbf{f}^{\mathcal{D}_j} \left(\mathbf{I}_i^{\mathcal{D}_j} \right) \right) \right], \left(\mathbf{I}_i^{\mathcal{D}_j}, \mathbf{y}_i^{\mathcal{D}_j} \right) \in \mathcal{D}_j, \quad (1)$$

where $\mathbf{f}^{\mathcal{D}_j}(\cdot)$ and $\mathbf{g}^{\mathcal{D}_j}(\cdot)$ are the corresponding feature extractor and classifier for \mathcal{D}_j , respectively. $\mathbf{y}_i^{\mathcal{D}_j}$ denotes the label of the image $\mathbf{I}_i^{\mathcal{D}_j}$. In this formulation, each dataset requires a specifically learned feature extractor for mapping $\mathbf{I}^{\mathcal{D}_j}$ to the target feature space. Due to the severe gap among the data distributions, the learned feature extractor is hard to transfer across different domains.

Assuming that the distributions of all datasets can be aligned, then the knowledge learned from these aligned distributions is supposed to generalize well on all aligned data. Based on this motivation, before learning and testing ReID algorithms, we propose to align the distributions of all the data, no matter from training or testing sets. Since the domain gap widely exists not only among datasets but also among cameras, we propose a camera-based formulation and align the distributions of all the data in a camera-wise manner. This formulation guarantees that the knowledge learned for some aligned cameras also applies to any other aligned cameras, regardless of the domains they belong to.

To align the distribution of each camera, we need to estimate the raw distribution of each camera and standardize images from each camera with the corresponding distribution statistics. We use $\boldsymbol{\eta}(c)$ to denote the estimated statistics related to the distribution of a training or testing camera c . Then, given an image $\mathbf{I}_i^{(c)}$ from this camera, aligning the camera distribution will transform this image as:

$$\mathcal{I}_i^{(c)} = \mathbf{DA} \left(\mathbf{I}_i^{(c)}; \boldsymbol{\eta}(c) \right), \quad (2)$$

where $\mathbf{DA}(\cdot)$ represents a distribution alignment mechanism, and $\mathcal{I}_i^{(c)}$ denotes the aligned $\mathbf{I}_i^{(c)}$. For any training set \mathcal{D}_j , we can now learn the ReID knowledge from this aligned distribution with the conventional training flows:

$$\arg \min \mathbb{E} \left[\mathbf{y}_i^{\mathcal{D}_j} - \mathbf{g}^{\mathcal{D}_j} \left(\mathbf{f} \left(\mathcal{I}_i^{(c)} \right) \right) \right], \left(\mathcal{I}_i^{(c)}, \mathbf{y}_i^{\mathcal{D}_j} \right) \in \mathcal{D}_j. \quad (3)$$

Note that the feature extractor $\mathbf{f}(\cdot)$ can be shared across all training and testing datasets, since the raw data from them has been aligned by $\mathbf{DA}(\cdot)$.

Bridge ReID Tasks. Considering that the major difference among ReID tasks is that they handle different combinations of training and testing sets, our formulation can connect and improve them all. For fully supervised learning and direct transfer, their difference lies in whether the training and testing sets belong to the same domain. Our formulation merges these two tasks because it always aligns the distribution of training and testing data. Meanwhile, by explicitly aligning the camera-related distributions, even with multiple training sets, the feature extractor $\mathbf{f}(\cdot)$ is still trained and tested under a similar distribution. This design reduces the knowledge forgetting caused by learning from different datasets and benefits the incremental learning. As for domain adaptation, aligning the camera-related distributions naturally shrinks the gap between the source training set and target training set. The knowledge learned from the source domain is more discriminative on the target domain, which helps to cluster unlabeled target images and predict more precise pseudo labels.

3.2. Camera-based Batch Normalization

To implement our camera-based formulation, we propose the Camera-based Batch Normalization (CBN) for aligning the distribution of each camera. CBN is modified from the conventional Batch Normalization [9], and estimate the camera-related statistics rather than the dataset-related statistics. In this section, we first go through the conventional Batch Normalization. Then, we elaborate CBN and the way of integrating it into ReID models.

Batch Normalization Revisited. The Batch Normalization layer [9] is designed to reduce the internal covariate shifting. During training, it standardizes the data in a mini-batch, records mini-batch mean and variance, and learns a transform that scales and shifts the standardized value. During testing, given an input \mathbf{x}_i , the output of the BN layer is:

$$\hat{\mathbf{x}}_i = \gamma \frac{\mathbf{x}_i - \hat{\boldsymbol{\mu}}}{\sqrt{\hat{\sigma}^2 + \epsilon}} + \beta, \quad (4)$$

where \mathbf{x}_i is the input and $\hat{\mathbf{x}}_i$ is the corresponding output. $\hat{\boldsymbol{\mu}}$ and $\hat{\sigma}^2$ are the overall mean and variance of the training set, which are approximated by the mini-batch mean and variance. γ and β are two parameters learned during training. Though the conventional BN stabilizes network training and brings performance improvements, its limitation lies in the assumption of data distribution. It assumes and requires that images from all testing sets are subject to the same distribution as the training set. Therefore, the conventional BN layer estimates the dataset-related statistics of the training set and directly uses the recorded values to standardize images from testing sets. However, for ReID models, this as-

sumption is only satisfied on the fully supervised learning task. On other ReID tasks, the distribution shifts of training and testing data lead to the failure of standardization and eventually damage the performance.

Batch Normalization within Cameras. To solve the above standardization inconsistency caused by BN, we design Camera-based Batch Normalization (CBN) to align the distribution of each camera. Unlike the conventional BN, CBN estimates the corresponding statistics for every training camera and testing camera independently. Therefore, CBN can well align the distributions of all cameras. Thus, the knowledge is always learned on the aligned distributions, making it better shared across all aligned cameras.

First, we describe how to align the camera-wise distribution. Given images or corresponding intermediate features $\mathbf{x}_m^{(c)}$ from camera c , the CBN layer standardizes them according to the statistics that relate to this camera:

$$\mu_{(c)} = \frac{1}{M} \sum_{m=1}^M \mathbf{x}_m^{(c)}, \quad (5)$$

$$\sigma_{(c)}^2 = \frac{1}{M} \sum_{m=1}^M \left(\mathbf{x}_m^{(c)} - \mu_{(c)} \right)^2, \quad (6)$$

$$\hat{\mathbf{x}}_m = \gamma \frac{\mathbf{x}_m - \mu_{(c)}}{\sqrt{\sigma_{(c)}^2 + \epsilon}} + \beta, \quad (7)$$

where $\mu_{(c)}$ and $\sigma_{(c)}^2$ denote the mean and variance related to this camera c . In the training stage, these two camera-related statistics are replaced by the batch-mean and batch-variance, *i.e.*, the same way in the conventional BN layers. During testing, before employing the learned ReID model to extract features, the above statistics have to be renewed for every testing camera. The details of approximating the overall camera-related statistics and generating the final features are presented in Algorithm 1. In short, we collect several unlabeled images per testing camera and calculate the corresponding camera-related statistics. Then, we employ these estimated statistics and previously trained model to generate the final features of testing images.

Next, we will carefully describe the details of training the ReID models embedded with our CBN. Note that the goal of ReID is to overcome the appearance variations across disjoint cameras. ReID models should be able to distinguish the appearance differences among cameras during training, *i.e.*, there should be images of the same identity captured by different cameras. Besides, our formulation uses batch-statistics to standardize the data from each camera. In each mini-batch, there should be multiple images for every involved camera so that the mini-batch mean and variance can be calculated. Following the above criterion, we design a sampling strategy that constructs a mini-batch with two steps. First, we randomly sample images and ensure that

Algorithm 1 Inference with CBN layers

Input: a trained feature extractor $\mathbf{f}(\cdot)$, images from the testing camera set \mathcal{C} .

Initialize: grouping testing images according to their camera ID and randomly samples N mini-batches from each group, denoted as $\{\mathbf{I}_i\}^{(c)}$

for all $c \leftarrow 1$ to $|\mathcal{C}|$ **do**

 Forward all images from $\{\mathbf{I}_i\}^{(c)}$ in N mini-batches

for all CBN layers in $\mathbf{f}(\cdot)$ **do**

 Collect the corresponding mini-batch mean μ_n and variance σ_n^2 and approximate the camera-wise mean $\hat{\mu}$ and variance $\hat{\sigma}^2$ for the current CBN layer:

$\hat{\mu}_{(c)} = \text{accumulate } \{\mu_1, \mu_2, \dots, \mu_N\}$

$\hat{\sigma}_{(c)}^2 = \text{accumulate } \{\sigma_1^2, \sigma_2^2, \dots, \sigma_N^2\}$

 Inject $\hat{\mu}_{(c)}$ and $\hat{\sigma}_{(c)}^2$ into the corresponding CBN layer

end for

for all images $\mathbf{I}^{(c)}$ from camera c **do**

 Compute final features $\mathbf{f}(\mathbf{I}^{(c)})$

end for

end for

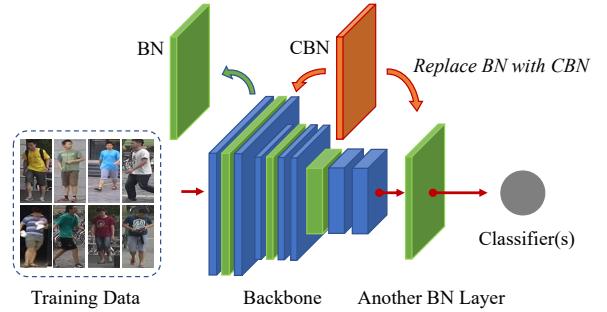


Figure 3. The visualization of our baseline network. Given an arbitrary backbone consisting of BN layers, we simply replace all BN layers with our CBN layers.

each sampled identity has exactly 4 images. Secondly, we filter the mini-batch to make sure that each involved camera has multiple images. The cameras with only one image are removed from the mini-batch. When training the ReID model with such a mini-batch, it should be kept in mind that only the standardization process is conducted per camera. All the other parameters in the network are trained with the data from all cameras.

3.3. Network Architecture

To demonstrate the advantage of our camera-based formulation over the conventional formulation, we use a barebones baseline, which only contains a deep neural network, an additional BN layer as the bottleneck, and fully connected layers as the classifiers. As shown in Fig. 3, our proposed camera-based formulation can be implemented by re-

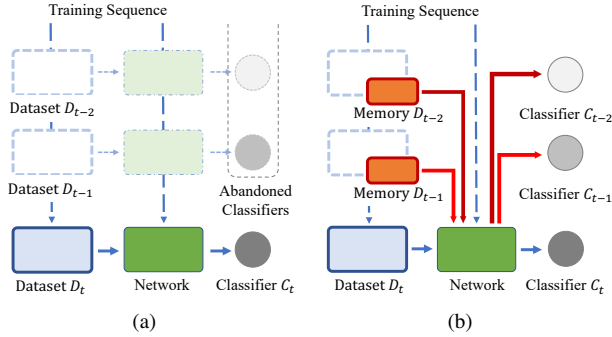


Figure 4. Visualizations of the two incremental learning settings involved in this paper. (a) **Data-Free**. (b) **Replay**. In the exemplar memory, each identity has one training image.

placing all BN layers with CBN layers. For all ReID tasks, each training set has a corresponding classifier. Therefore, for the tasks that involve multiple training sets, there will be multiple classifiers in our framework.

Along with the widely studied tasks of fully supervised learning, direct transfer, and domain adaptation, we also evaluate our method on the incremental learning task, which is rarely discussed in the ReID community. Incremental learning studies the problem of learning knowledge incrementally from a sequence of training sets while preserving the previously learned knowledge. Therefore, incremental learning needs to handle multiple training sets. As shown in Fig. 4, we propose two experiment settings. First, the **Data-Free** mode. Once we finish the training procedure on a dataset, the data along with the corresponding classifiers are abandoned. When training the model on the subsequent training sets, the old data will never show up again. Second, the **Replay** mode. Unlike the Data-Free mode, we construct an exemplar set from each old training set. The exemplar set and the corresponding classifier are preserved during the entire training sequence. When training the ReID model on a new dataset, exemplars and the classifiers are used along with the latest data and classifiers.

3.4. Difference from Previous Work

A previous work that closely relates to our method is CamStyle [50], which noticed the style difference among cameras and transferred the image style in a camera-to-camera manner. However, it not only brought noises to the transferred images but also had to retrain the model on the new generated distribution. Differently, our work targets to align the domain distribution of each camera, and the ReID knowledge learned from the aligned distributions can be shared on each aligned camera. Moreover, compared to CamStyle, our method is easy to implement and nearly cost-free. AdaBN [15] is another work that inspired us. It aligned the distribution of the entire training domain and target domain. However, in ReID tasks, it is hard to align

the distributions of different datasets because the dataset-related distribution is sensitive to camera variations.

4. Experiments

4.1. Datasets

In this paper, we utilize three large scale ReID datasets, including Market-1501 [43], DukeMTMC-reID [45], and MSMT17 [39]. Market-1501 dataset has 1,501 identities in total, among which 751 identities are used for training and the rest for testing. The training set contains 12,936 images and the testing set contains 15,913 images collected from 6 outdoor cameras. DukeMTMC-reID dataset contains 16,522 images of 702 identities for training, and other 1,110 identities with 17,661 images are used for testing. The images are captured from 8 cameras. MSMT17 dataset is the current largest ReID dataset with 126,441 images of 4,101 identities from 15 cameras. MSMT17 is a challenging dataset since it covers much more complicated scenarios and is collected in a long-time period, which leads to diverse illumination conditions. For short, we denote Market-1501 as Market, DukeMTMC-reID as Duke, and MSMT17 as MSMT in the rest of this paper. It is worth noting that for each of these datasets, the training and testing subsets contain the same camera combinations. Thus, the dataset-based distribution is similar between these two subsets.

4.2. Implementation Details

In this paper, all experiments are conducted with PyTorch. In both training and testing, the size of input images is 256×128 , and the batch size is 64. The baseline network presented in Sec. 3.3 uses the ResNet-50 [7] as the backbone. To train this network, we adopt SGD optimizer with momentum [26] of 0.9 and weight decay of 5×10^{-4} . Moreover, the initial learning rate is 0.01, and it decays after the 40th epoch by a factor of 10. For all experiments, the training stage will end up with 60 epochs. It is worth noting that we utilize a warm-up stage for incremental learning. In the warm-up stage, we freeze the backbone and only fine-tune the classifier(s) to avoid damaging the previously learned knowledge. More details are shown in supplementary materials. During testing, our framework will first sample a few unlabeled images from each camera and use them to approximate the camera-related statistics. Then, these statistics are fixed and employed to process the corresponding testing images. Following the conventions, mean Average Precision (mAP) and Cumulative Matching Characteristic (CMC) curves are utilized for evaluations.

4.3. Performance on Different ReID Tasks

We evaluate our proposed methods on four types of ReID tasks, *i.e.*, fully supervised learning, direct transfer, domain adaptation, and incremental learning. For fair comparisons

Training Set	Testing Set	Market			Duke			MSMT		
	Method	rank-1	rank-10	mAP	rank-1	rank-10	mAP	rank-1	rank-10	mAP
Market	Baseline	90.2	97.9	74.0	37.0	58.9	20.7	17.1	31.4	5.5
	Ours	91.3	98.4	77.3	58.7	78.1	38.2	25.3	43.3	9.5
Duke	Baseline	53.2	76.0	25.1	81.5	94.0	66.6	27.2	44.7	9.1
	Ours	72.7	90.7	43.0	82.5	94.1	67.3	35.4	54.6	13.0
MSMT	Baseline	58.1	79.7	30.8	57.8	78.3	38.4	71.5	86.6	42.3
	Ours	73.7	91.1	45.0	66.2	83.6	46.7	72.8	87.2	42.9

Table 1. Results of the baseline method with our formulation and the conventional formulation. The fully supervised learning results are in *italics*. Unless otherwise stated, the **baseline** method in the following sections refers to the method described in Sec. 3.3.

Method	Market			
	rank-1	rank-5	rank-10	mAP
SVDNet [34]	82.3	92.3	95.2	62.1
CamStyle [50]	88.1	-	-	68.7
VCFL [18]	89.3	-	-	74.5
MLFN [2]	90.0	-	-	74.3
MaskReID [25]	90.0	-	-	75.3
SCPNet [5]	91.2	97.0	-	75.2
HA-CNN [14]	91.2	-	-	75.7
PGFA [23]	91.2	-	-	76.8
MVP [33]	91.4	-	-	80.5
SGGNN [28]	92.3	96.1	97.4	82.8
SPReID [11]	92.5	97.2	98.1	81.3
BoT* [21]	93.6	97.6	98.4	82.2
PCB+RPP [35]	93.8	97.5	98.5	81.6
Baseline	90.2	96.7	97.9	74.0
Ours+Baseline	91.3	97.1	98.4	77.3
Ours+BoT*	94.3	97.9	98.7	83.6

Table 2. Results of the state-of-the-art fully supervised learning methods. All models are trained and tested on Market. BoT* denotes our results with the official BoT code. In BoT*, Random Erasing is disabled due to its negative effect on direct transfer.

with the previous methods, we always utilize the same network architecture and training strategy for each comparison. Details are introduced below.

4.3.1 Fully Supervised Learning and Direct Transfer

Fully supervised learning aims at evaluating how well a ReID model fits the given scenario, and the direct transfer focuses on demonstrating the generalization ability of the learned ReID model. Therefore, the difference between them only lies in whether the testing set is sampled from the same scenario as the training set. Since all the other settings are the same, we evaluate these two tasks together.

Note that we focus on demonstrating the effectiveness of our camera-based formulation, so we utilize the bare-bones network presented in Sec. 3.3 for clarity. As shown in Table 1, our proposed method shows good advantages, *e.g.*, there is an average 1.1% improvement in rank-1 accuracy

Method	Duke			
	rank-1	rank-5	rank-10	mAP
CamStyle [50]	75.3	-	-	53.5
SVDNet [34]	76.7	86.4	89.9	56.8
MaskReID [25]	78.8	-	-	61.9
SCPNet [5]	80.3	89.6	-	62.6
HA-CNN [14]	80.5	-	-	63.8
MLFN [2]	81.0	-	-	62.8
SGGNN [28]	81.1	88.4	91.2	68.2
PGFA [23]	82.6	-	-	65.5
PCB+RPP [35]	83.3	90.5	92.5	69.2
MVP [33]	83.4	-	-	70.0
BoT* [21]	84.3	91.9	94.2	70.1
SPReID [11]	84.4	91.9	93.7	71.0
Baseline	81.5	91.4	94.0	66.6
Ours+Baseline	82.5	91.7	94.1	67.3
Ours+BoT*	84.8	92.5	95.2	70.1

Table 3. Results of the state-of-the-art fully supervised learning methods. All models are trained and tested on Duke.

for the fully supervised learning task. Meanwhile, without bells and whistles, there is an average 13.6% improvement in rank-1 accuracy for the direct transfer task. We recognize that our method has to collect a few unlabeled samples from each testing camera for estimating the camera-related statistics. However, this process is fast and nearly free. To further demonstrate our proposed method, we also conduct experiments on domain adaptation. The corresponding results are presented in Sec. 4.3.2.

Besides, our proposed formulation can be easily integrated into many ReID methods and boosts their performance. Take BoT [21], a recent state-of-the-art method in fully supervised learning, as an example. We integrate our proposed CBN into BoT and conduct experiments with almost the same settings as in the original paper, including the network architecture, objective functions, and training strategies. The only difference is that we disable Random Erasing [47] due to its constant negative effects on direct transfer. The results of the fully supervised learning on Market and Duke are shown in Table 2 and Table 3, re-

Method	Duke to Market			
	rank-1	rank-5	rank-10	mAP
UMDL [24]	34.5	52.6	59.6	12.4
PTGAN [39]	38.6	-	66.1	-
PUL [4]	45.5	60.7	66.7	20.5
SPGAN [3]	51.5	70.1	76.8	22.8
BoT* [‡] [21]	53.3	69.7	76.4	24.9
MMFA [17]	56.7	75.0	81.8	27.4
TJ-AIDL [38]	58.2	74.8	81.1	26.5
CamStyle [50]	58.8	78.2	84.3	27.4
HHL [48]	62.2	78.8	84.0	31.4
ECN [49]	75.1	87.6	91.6	43.0
Baseline [‡]	53.2	70.0	76.0	25.1
Ours+BoT* [‡]	68.6	82.5	87.7	39.0
Ours+Baseline [‡]	72.7	85.8	90.7	43.0
Ours+ECN	81.7	91.9	94.7	52.0

Table 4. The results of testing ReID models across datasets. These results denote transferring models from Duke to Market. [‡] marks methods that only use the source domain data for training.

spectively. It should be pointed out that in fully supervised learning, the training and testing set are sampled from the same camera set. Therefore, there is no significant shift among the BN statistics of the training set and the testing set, which favors the conventional formulation. Even so, our method still slightly improves the performance on both Market and Duke, which clearly demonstrates the effectiveness of learning in a camera-wise manner. Moreover, we also present the results on direct transfer in Table 4 and Table 5. It is clear that our method improves BoT significantly, *e.g.*, there is a 15.3% rank-1 improvement when training on Duke but testing on Market. These improvements on both fully supervised learning and direct transfer show the advantages of our camera-based formulation.

4.3.2 Domain Adaptation

To better evaluate our proposed methods, we further conduct experiments on domain adaptation, which usually involves a labeled source training set and another unlabeled target training set. The results are shown in Table 4 and Table 5. Our method surpasses most domain adaptation methods using only the source domain for training. Moreover, we integrate our formulation into a recent domain adaptation method ECN [49] and conduct experiments between two ReID datasets. By learning ReID knowledge from aligned distributions of source domains and target domains, the performance of ECN is significantly boosted, *e.g.*, when transferring from Duke to Market, the rank-1 accuracy and mAP are improved by 6.6% and 9.0%, respectively. These improvements clearly demonstrate the effectiveness of our camera-based formulation on the domain adaptation task.

Method	Market to Duke			
	rank-1	rank-5	rank-10	mAP
UMDL [24]	18.5	31.4	37.6	7.3
PTGAN [39]	27.4	-	50.7	-
PUL [4]	30.0	43.4	48.5	16.4
SPGAN [3]	41.1	56.6	63.0	22.3
BoT* [‡] [21]	43.9	58.8	64.9	26.1
MMFA [17]	45.3	59.8	66.3	24.7
TJ-AIDL [38]	44.3	59.6	65.0	23.0
HHL [48]	46.9	61.0	66.7	27.2
CamStyle [50]	48.4	62.5	68.9	25.1
ECN [49]	63.3	75.8	80.4	40.4
Baseline [‡]	37.0	52.6	58.9	20.7
Ours+Baseline [‡]	58.7	74.1	78.1	38.2
Ours+BoT* [‡]	60.6	74.0	78.5	39.8
Ours+ECN	68.0	80.0	83.9	44.9

Table 5. The results of testing ReID models across datasets. These results denote transferring models from Market to Duke. [‡] marks methods that only use the source domain data for training.

4.3.3 Incremental Learning

Incremental learning is an application that handles multiple training sets. Learning ReID models incrementally is vital for real-world applications because usually, only part of all training data is available at a time. The major problem of incremental learning is Catastrophic Forgetting, *i.e.*, when learning on new datasets, models tend to forget the previously learned knowledge. Since our formulation learns the ReID model in the aligned distributions, it can significantly reduce Catastrophic Forgetting.

To demonstrate our advantages, we design the experiments as follows. Given three large-scale ReID datasets, there are in total six training sequences of length 2, such as (Market→Duke) and six sequences of length 3, such as (Market→Duke→MSMT). We use the baseline method described in Sec. 3.3 and train it on all sequences separately. After training on each dataset of every sequence, we evaluate the latest model on the first dataset of the corresponding sequence and record the performance decreases. As described in Sec. 3.3, both the **Data-Free** and the **Replay** settings are tested here. For the Replay settings, the exemplars are selected by randomly sampling one image for each identity. In this way, compared to the original training sets, the size of the exemplar set for Market, Duke, and MSMT is only 5.5%, 4.2%, and 3.4%, respectively. More details for selecting exemplars are given in supplementary materials.

The corresponding results are shown in Table 6. For better demonstrating our improvements, we report the averaged results of the sequences that are of the same length and share the same initial dataset, *e.g.*, averaging the results of testing Market on the sequences Market→Duke and Market→MSMT. In short, our formulation outperforms the

Testing Set		Market			Duke			MSMT		
Seq Length	Methods	rank-1	rank-10	mAP	rank-1	rank-10	mAP	rank-1	rank-10	mAP
1	-	100%	100%	100%	100%	100%	100%	100%	100%	100%
2	Baseline [§]	82.2%	93.3%	62.5%	80.2%	88.4%	68.8%	55.5%	68.1%	38.7%
	Ours [§]	88.3%	96.0%	71.2%	89.3%	94.4%	83.2%	74.5%	82.9%	58.9%
	Baseline [†]	92.5%	98.1%	84.1%	90.9%	94.7%	84.7%	81.7%	89.7%	70.1%
	Ours [†]	95.0%	98.2%	85.7%	94.3%	96.8%	91.1%	91.6%	95.0%	84.6%
3	Baseline [§]	74.8%	89.1%	52.2%	75.2%	85.4%	63.0%	38.9%	53.1%	24.7%
	Ours [§]	85.8%	94.9%	66.0%	85.8%	91.9%	77.4%	56.6%	69.2%	39.4%
	Baseline [†]	86.5%	95.5%	74.0%	84.1%	90.4%	76.4%	74.3%	84.1%	60.9%
	Ours [†]	94.4%	98.0%	83.1%	91.5%	95.4%	87.6%	86.4%	91.1%	76.0%

Table 6. Results of ReID models on incremental learning tasks. Each result denotes the percentage of the performance preserved on the first dataset after learning on new datasets. § marks the Data-Free incremental learning. † corresponds to the Replay incremental learning.

Training Method	Testing Method	Market to Market		Market to Duke		Duke to Duke		Duke to Market	
		rank-1	mAP	rank-1	mAP	rank-1	mAP	rank-1	mAP
BN	BN	90.2	74.0	37.0	20.7	81.5	66.6	53.2	25.1
BN	AdaBN [15]	89.6	73.7	43.0	26.3	81.2	66.2	55.8	28.1
BN	Our CBN	89.5	73.4	55.9	34.9	80.2	63.7	69.5	40.6
Our CBN	Our CBN	91.3	77.3	58.7	38.2	82.5	67.3	72.7	43.0

Table 7. Results of combining different normalization strategies in the fully supervised learning and direct transfer.

Batches	mAP	Fully Supervised		Direct Transfer	
		mean	var	mean	var
1		76.29	0.032	37.34	0.047
5		77.21	0.010	38.08	0.017
10		77.33	0.007	38.19	0.008
20		77.37	0.005	38.18	0.002
50		77.39	0.001	38.21	0.001

Table 8. The mAP of our method on the above two tasks. The training set is Market, and testing sets are Market and Duke.

conventional formulation in all experiments. These results further demonstrate the effectiveness of our formulation.

4.4. Discussion

All experiments demonstrate that our camera-based formulation boosts most of the ReID tasks. However, there are two remaining questions that should be figured out.

First, given a trained ReID model with the conventional batch normalization (BN), can we directly test it with our camera-based batch normalization (CBN)? In the conventional BN, the statistics recorded from the entire training set are directly used for standardizing testing images, while our CBN uses the camera-related statistics. To evaluate it, we compare different combinations of normalization strategies. As shown in Table 7, when directly utilizing CBN to test a conventional BN model, the performance gets better on the direct transfer but worse on the fully supervised learning. Only when using our CBN in both the training and testing stage, the performance of all listed tasks is improved.

Besides, our method also outperforms AdaBN [15], which estimates and aligns the distribution of the entire dataset.

Second, for our camera-based formulation, how many samples are required for approximating the camera-related statistics in the testing stage? We conduct experiments on different numbers of samples. Note that if a camera contains less than the required number of images, we simply use all available images rather than duplicate them. For reliability, we repeat all experiments 10 times and report the averaged results in Table 8. As demonstrated, the performance is better and more stable when using more samples to estimate the camera-related statistics. Besides, the results are already good enough when only utilizing very few samples, *e.g.*, 10 mini-batches. For the balance of simplicity and performance, we adopt 10 mini-batches to estimate the camera-related BN statistics in all above experiments.

5. Conclusion

This paper reveals the inherent cause that isolates different ReID topics. We propose a generic camera-based formulation that connects and improves multiple isolated ReID topics. Through our implementation, *i.e.*, Camera-based Batch Normalization, we align the distribution of all training and testing cameras and guarantee that the ReID knowledge is always learned, accumulated, and verified in the aligned distributions. Comprehensive experiments demonstrate the effectiveness of our method on multiple ReID tasks. Moreover, thanks to its ability to handle cameras from arbitrary scenarios, our formulation also paves the way towards fast deployment of ReID systems in the real world.

Appendix

A. The Warm-Up Strategy in Section 4.2

In this section, we describe the warm-up strategy for initializing fully-connected classifiers in incremental learning tasks. Given a model that has already been trained on one or multiple ReID datasets, when fine-tuning it on a new training set, a new fully-connected classifier for classifying images from this specific dataset is required. Since this classifier is randomly initialized, if we directly fine-tune the entire model in an end-to-end manner, this classifier will introduce lots of noises to the feature extractor and heavily damage the previously learned knowledge. To alleviate the knowledge forgetting in the early stage of training, we warm-up the newest classifier before the formal training. Note that in the Replay incremental learning, there could be classifiers and images that correspond to multiple training sets (the exemplar memory and the current training set). However, in the warm-up stage of all incremental learning tasks, we only consider the latest training set and the corresponding new classifier. The details of this warm-up strategy are presented in Algorithm 2. In short, we only iteratively fine-tune the new classifier on the latest training set until the loss becomes stable. After the warm-up stage, we start to train the entire network in a conventional end-to-end manner.

Algorithm 2 Warm-up the latest classifier

Input: a trained ReID model with the feature extractor $\mathbf{f}(\cdot)$, image \mathbf{I}_i and the corresponding ID \mathbf{y}_i from the latest training set \mathcal{D}

Initialize: freeze all trainable parameters in $\mathbf{f}(\cdot)$, randomly initialize a new classifier $\mathbf{g}(\cdot)$ for \mathcal{D} , set counter $n = 0$, set an empty list $\mathcal{L} = []$

repeat

Randomly sample a mini-batch $\{\mathbf{I}_i\}$ and the corresponding $\{\mathbf{y}_i\}$ from \mathcal{D}

$\mathcal{L} = \text{get_loss}(\mathbf{g}(\mathbf{f}(\{\mathbf{I}_i\})), \{\mathbf{y}_i\})$

Backward \mathcal{L} and only update $\mathbf{g}(\cdot)$

Append \mathcal{L} to \mathcal{L}

Truncate \mathcal{L} and only preserve the latest 50 items

if (\mathcal{L} has 50 items) & ($|\mathcal{L} - \text{mean}(\mathcal{L})| \leq 0.1$) **then**
 $n = n + 1$

else

$n = 0$

end if

until $n = 5$

B. Exemplar Memory in Section 4.3.3

The exemplar memory is built for the Replay incremental learning task. Its goal is to reinforce the discriminative knowledge of the previous training sets with the least

Algorithm 3 Build the exemplar memory

Input: a ReID set \mathcal{D} with \mathcal{N} identities and \mathcal{C} cameras

Output: the exemplar memory \mathcal{M} in which each identity from \mathcal{D} has exactly one image

Initialize: create a dict Ω that records the number of already picked images from each camera.

for all identity n in \mathcal{N} **do**

Collect all images that belong to the identity n

Collect the camera ID of the above images as $\{c\}$

Query Ω with $\{c\}$ and find the camera c that has the least picked images

Randomly pick an image that simultaneously belongs to camera c and identity n , and add it to \mathcal{M}

$\Omega[c] = \Omega[c] + 1$

end for

amount of old images. In this paper, we design a straightforward approach to achieve this goal. For each old training set, we propose a greedy algorithm that saves one image for each identity and tries to keep an equal number of images for each old camera. The details are presented in Algorithm 3. With this approach, the size of the exemplar memory for Market [43], Duke [45], and MSMT17 [39] is only 5.5%, 4.2%, and 3.4% of their original training set, respectively.

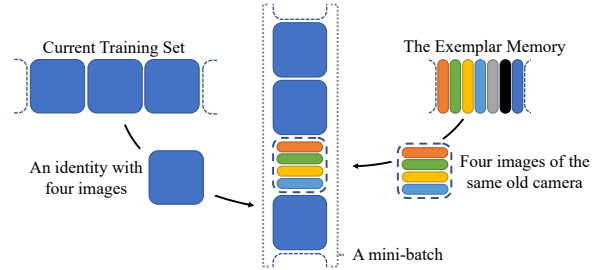


Figure 5. The demonstration of a mini-batch. (1) A blue rectangle denotes four images of the same identity. The methods for sampling these images are stated in Section 3.2. (2) The rectangles in other colors represent the images from the exemplar memory. Each rectangle corresponds to one image of an old identity. We group these exemplars according to their camera ID, and randomly fuse these groups with the data sampled from the current training set.

Another thing worth noting is the way of utilizing these exemplars together with the data from the latest training set. On the one hand, in the exemplar memory, there are only very few samples that describe the previous cameras, and each old identity only has one image. On the other hand, as described in Section 3.2, for the latest training set, each identity has multiple images in the mini-batch, so does each camera. To make sure that our method can accurately approximate the CBN statistics of all previous and current cameras, we design a mixed sampling strategy. As shown

in Fig. 5, when handling images from the latest training set, we follow the pipeline presented in Section 3.2. When sampling identities from the exemplar memory, we cluster images from the exemplar memory and make sure that each group has four successive old images that correspond to the same old camera. Then, these groups are randomly fused with the images sampled from the latest training set.

References

- [1] Jon Almazan, Bojana Gajic, Naila Murray, and Diane Larlus. Re-id done right: towards good practices for person re-identification. *arXiv preprint arXiv:1801.05339*, 2018.
- [2] Xiaobin Chang, Timothy M Hospedales, and Tao Xiang. Multi-level factorisation net for person re-identification. In *CVPR*. IEEE, 2018.
- [3] Weijian Deng, Liang Zheng, Qixiang Ye, Guoliang Kang, Yi Yang, and Jianbin Jiao. Image-image domain adaptation with preserved self-similarity and domain-dissimilarity for person re-identification. In *CVPR*. IEEE, 2018.
- [4] Hehe Fan, Liang Zheng, Chenggang Yan, and Yi Yang. Unsupervised person re-identification: Clustering and fine-tuning. *ACM Transactions on Multimedia Computing, Communications, and Applications (TOMM)*, 14(4):83, 2018.
- [5] Xing Fan, Hao Luo, Xuan Zhang, Lingxiao He, Chi Zhang, and Wei Jiang. Scpnnet: Spatial-channel parallelism network for joint holistic and partial person re-identification. In *ACCV*. Springer, 2018.
- [6] Yang Fu, Yunchao Wei, Guanshuo Wang, Yuqian Zhou, Honghui Shi, and Thomas S Huang. Self-similarity grouping: A simple unsupervised cross domain adaptation approach for person re-identification. In *ICCV*. IEEE, 2019.
- [7] Kaiming He, Xiangyu Zhang, Shaoqing Ren, and Jian Sun. Deep residual learning for image recognition. In *CVPR*. IEEE, 2016.
- [8] Houjing Huang, Wenjie Yang, Xiaotang Chen, Xin Zhao, Kaiqi Huang, Jinbin Lin, Guan Huang, and Dalong Du. Eanet: Enhancing alignment for cross-domain person re-identification. *arXiv preprint arXiv:1812.11369*, 2018.
- [9] Sergey Ioffe and Christian Szegedy. Batch normalization: Accelerating deep network training by reducing internal covariate shift. *arXiv preprint arXiv:1502.03167*, 2015.
- [10] Jiening Jiao, Wei-Shi Zheng, Ancong Wu, Xiatian Zhu, and Shaogang Gong. Deep low-resolution person re-identification. In *AAAI*, 2018.
- [11] Mahdi M Kalayeh, Emrah Basaran, Muhittin Gökmen, Mustafa E Kamasak, and Mubarak Shah. Human semantic parsing for person re-identification. In *CVPR*. IEEE, 2018.
- [12] James Kirkpatrick, Razvan Pascanu, Neil Rabinowitz, Joel Veness, Guillaume Desjardins, Andrei A Rusu, Kieran Milan, John Quan, Tiago Ramalho, Agnieszka Grabska-Barwinska, et al. Overcoming catastrophic forgetting in neural networks. *Proceedings of the national academy of sciences*, 114(13):3521–3526, 2017.
- [13] Wei Li, Xiatian Zhu, and Shaogang Gong. Harmonious attention network for person re-identification. In *CVPR*. IEEE, 2018.
- [14] Wei Li, Xiatian Zhu, and Shaogang Gong. Harmonious attention network for person re-identification. In *CVPR*. IEEE, 2018.
- [15] Yanghao Li, Naiyan Wang, Jianping Shi, Jiaying Liu, and Xiaodi Hou. Revisiting batch normalization for practical domain adaptation. *arXiv preprint arXiv:1603.04779*, 2016.
- [16] Zhizhong Li and Derek Hoiem. Learning without forgetting. *IEEE Transactions on Pattern Analysis and Machine Intelligence*, 40(12):2935–2947, 2018.
- [17] Shan Lin, Haoliang Li, Chang-Tsun Li, and Alex Chichung Kot. Multi-task mid-level feature alignment network for unsupervised cross-dataset person re-identification. In *BMVC*, 2018.
- [18] Fangyi Liu and Lei Zhang. View confusion feature learning for person re-identification. In *ICCV*. IEEE, 2019.
- [19] Hao Liu, Jiashi Feng, Meibin Qi, Jianguo Jiang, and Shuicheng Yan. End-to-end comparative attention networks for person re-identification. *IEEE Transactions on Image Processing*, 26(7):3492–3506, 2017.
- [20] Jinxian Liu, Bingbing Ni, Yichao Yan, Peng Zhou, Shuo Cheng, and Jianguo Hu. Pose transferrable person re-identification. In *CVPR*. IEEE, 2018.
- [21] Hao Luo, Youzhi Gu, Xingyu Liao, Shenqi Lai, and Wei Jiang. Bag of tricks and a strong baseline for deep person re-identification. In *CVPRW*, 2019.
- [22] Shunan Mao, Shiliang Zhang, and Ming Yang. Resolution-invariant person re-identification. *arXiv preprint arXiv:1906.09748*, 2019.
- [23] Jiaxu Miao, Yu Wu, Ping Liu, Yuhang Ding, and Yi Yang. Pose-guided feature alignment for occluded person re-identification. In *ICCV*. IEEE, 2019.
- [24] Peixi Peng, Tao Xiang, Yaowei Wang, Massimiliano Pontil, Shaogang Gong, Tiejun Huang, and Yonghong Tian. Unsupervised cross-dataset transfer learning for person re-identification. In *CVPR*. IEEE, 2016.
- [25] Lei Qi, Jing Huo, Lei Wang, Yinghuan Shi, and Yang Gao. Maskreid: A mask based deep ranking neural network for person re-identification. In *ICME*, 2019.
- [26] Ning Qian. On the momentum term in gradient descent learning algorithms. *Neural networks*, 12(1):145–151, 1999.
- [27] Amal Rannen, Rahaf Aljundi, Matthew B Blaschko, and Tinne Tuytelaars. Encoder based lifelong learning. In *ICCV*. IEEE, 2017.
- [28] Yantao Shen, Hongsheng Li, Shuai Yi, Dapeng Chen, and Xiaogang Wang. Person re-identification with deep similarity-guided graph neural network. In *ECCV*. IEEE, 2018.
- [29] Chunfeng Song, Yan Huang, Wanli Ouyang, and Liang Wang. Mask-guided contrastive attention model for person re-identification. In *CVPR*. IEEE, 2018.
- [30] Jifei Song, Yongxin Yang, Yi-Zhe Song, Tao Xiang, and Timothy M Hospedales. Generalizable person re-identification by domain-invariant mapping network. In *CVPR*. IEEE, 2019.
- [31] Liangchen Song, Cheng Wang, Lefei Zhang, Bo Du, Qian Zhang, Chang Huang, and Xinggang Wang. Unsupervised domain adaptive re-identification: Theory and practice. *arXiv preprint arXiv:1807.11334*, 2018.

- [32] Yumin Suh, Jingdong Wang, Siyu Tang, Tao Mei, and Kyoung Mu Lee. Part-aligned bilinear representations for person re-identification. In *ECCV*. Springer, 2018.
- [33] Han Sun, Zhiyuan Chen, Shiyang Yan, and Lin Xu. Mvp matching: A maximum-value perfect matching for mining hard samples, with application to person re-identification. In *ICCV*. IEEE, 2019.
- [34] Yifan Sun, Liang Zheng, Weijian Deng, and Shengjin Wang. Svdnet for pedestrian retrieval. In *ICCV*. IEEE, 2017.
- [35] Yifan Sun, Liang Zheng, Yi Yang, Qi Tian, and Shengjin Wang. Beyond part models: Person retrieval with refined part pooling (and a strong convolutional baseline). In *ECCV*, 2018.
- [36] Maoqing Tian, Shuai Yi, Hongsheng Li, Shihua Li, Xuesen Zhang, Jianping Shi, Junjie Yan, and Xiaogang Wang. Eliminating background-bias for robust person re-identification. In *CVPR*. IEEE, 2018.
- [37] Laurens Van Der Maaten. Accelerating t-sne using tree-based algorithms. *JMLR*, 15(1):3221–3245, 2014.
- [38] Jingya Wang, Xiatian Zhu, Shaogang Gong, and Wei Li. Transferable joint attribute-identity deep learning for unsupervised person re-identification. In *CVPR*. IEEE, 2018.
- [39] Longhui Wei, Shiliang Zhang, Wen Gao, and Qi Tian. Person transfer gan to bridge domain gap for person re-identification. In *CVPR*. IEEE, 2018.
- [40] Longhui Wei, Shiliang Zhang, Hantao Yao, Wen Gao, and Qi Tian. Glad: Global-local-alignment descriptor for pedestrian retrieval. In *ACMMM*. ACM, 2017.
- [41] Ancong Wu, Wei-Shi Zheng, Xiaowei Guo, and Jian-Huang Lai. Distilled person re-identification: Towards a more scalable system. In *CVPR*. IEEE, 2019.
- [42] Xuan Zhang, Hao Luo, Xing Fan, Weilai Xiang, Yixiao Sun, Qiqi Xiao, Wei Jiang, Chi Zhang, and Jian Sun. Alignedreid: Surpassing human-level performance in person re-identification. *arXiv preprint arXiv:1711.08184*, 2017.
- [43] Liang Zheng, Liyue Shen, Lu Tian, Shengjin Wang, Jingdong Wang, and Qi Tian. Scalable person re-identification: A benchmark. In *ICCV*. IEEE, 2015.
- [44] Zhedong Zheng, Liang Zheng, and Yi Yang. A discriminatively learned cnn embedding for person reidentification. *ACM Transactions on Multimedia Computing, Communications, and Applications*, 14(1):13, 2017.
- [45] Zhedong Zheng, Liang Zheng, and Yi Yang. Unlabeled samples generated by gan improve the person re-identification baseline in vitro. In *ICCV*. IEEE, 2017.
- [46] Zhun Zhong, Liang Zheng, Donglin Cao, and Shaozi Li. Re-ranking person re-identification with k-reciprocal encoding. In *CVPR*. IEEE, 2017.
- [47] Zhun Zhong, Liang Zheng, Guoliang Kang, Shaozi Li, and Yi Yang. Random erasing data augmentation. *arXiv preprint arXiv:1708.04896*, 2017.
- [48] Zhun Zhong, Liang Zheng, Shaozi Li, and Yi Yang. Generalizing a person retrieval model hetero-and homogeneously. In *ECCV*. Springer, 2018.
- [49] Zhun Zhong, Liang Zheng, Zhiming Luo, Shaozi Li, and Yi Yang. Invariance matters: Exemplar memory for domain adaptive person re-identification. In *CVPR*. IEEE, 2019.
- [50] Zhun Zhong, Liang Zheng, Zhedong Zheng, Shaozi Li, and Yi Yang. Camera style adaptation for person re-identification. In *CVPR*. IEEE, 2018.
- [51] Jiahuan Zhou, Pei Yu, Wei Tang, and Ying Wu. Efficient online local metric adaptation via negative samples for person reidentification. In *ICCV*. IEEE, 2017.
- [52] Jun-Yan Zhu, Taesung Park, Phillip Isola, and Alexei A Efros. Unpaired image-to-image translation using cycle-consistent adversarial networks. In *ICCV*. IEEE, 2017.